

Measured and Calculated Static Equilibrium Position of Water-lubricated Tilting-pad Journal Bearing

J. Pokorný^{1,*}, T. Návrat¹

¹ *Institute of Solid Mechanics, Mechatronics and Biomechanics, Faculty of Mechanical Engineering, Brno University of Technology, Technická 2896, 616 69 Brno, Czech Republic*

* *jan.pokorny4@vutbr.cz*

Abstract: This paper deals with the measurement and computational modelling of the static equilibrium position of the hydrodynamic water-lubricated tilting-pad journal bearing. The measurement is carried out on a developed test rig with two bearing housings. A computational model is presented based on the generalized Reynolds equation coupled with the 2D energy equation in the bearing mid-plane. This model includes the lubricant mixing, deformation and tilting of the pads. The steady-state solution is reached using the finite volume method. To find the static equilibrium position of the bearing, the Anderson method with bounds is implemented. Results of the equilibrium position in dependence on the journal speed are given for a particular water-lubricated journal bearing. These results are validated with the measured data.

Keywords: tilting pad journal bearing; water lubricated; measurement; numerical analysis; static equilibrium.

1 Introduction

The knowledge of the static equilibrium position of the hydrodynamic tilting-pad journal bearing is the basis for the determination of its static and dynamic performance. Therefore, it is necessary to establish this equilibrium position. A tilting-pad bearing is in the static equilibrium position if the force balance between the external load and the hydrodynamic pressure resultant and the moment balance of all the pads to their pivots are satisfied at the same time [1]. This position can be determined experimentally or by computational modelling.

The beginning of computational modelling can be dated back to 1886 when O. Reynolds gave the basis for the theory of the thin lubricant film [2]. Since then, many scientists have worked on this problem and the theory has been modified to incorporate some other effects. These effects include the consideration of variable viscosity depending on temperature, which led to the development of the generalized Reynolds equation [3]. Furthermore, the effect of turbulence has been involved using turbulence coefficients [4]. Mixing of hot and cold lubricant in the lubricant grooves has been proposed by Heshmat and Pinkus [5]. The accuracy of the computational models has also increased by considering the deformation and tilting of the pads [6]. However, Reynolds' basis remains.

To calculate the equilibrium position, root-finding methods are used. These methods have been divided into three groups by the author [1]. The first one includes the bisection method, which was used to determine the equilibrium position of lemon-bore bearings by the author [7], or the twofold secant method for tilting-pad bearings published by Zhou et al. [8]. The second group contains optimization methods, for example, the multiple directions method [9]. The third group comprises the Newton-Raphson method used e.g. in [10] but also the very efficient bounded quasi-Newton methods proposed by the author [1].

For the validation of the computational model, a comparison of the computational results with the experiment is preferably performed. The measurement of the equilibrium position has been addressed by many authors, e.g. [11–13].

2 Methods

2.1 Test rig and instrumentation

Fig. 1 shows a test rig for measuring the static performance of the hydrodynamic journal bearings. This device consists of a rigid frame allowing axial displacement of all components and ensuring their correct alignment. The frame is fitted with two bearing housings containing water-lubricated hydrodynamic tilting-pad journal bearings. A rigid rotor is mounted in these bearings, which is driven by a high-speed electric motor up to 18,000 rpm via a flexible coupling. The stiffness of the device is increased by two crossbars, on which four eddy current proximity probes are placed near the bearing housings for measuring rotor displacements relatively to the housings. The rotor speed is measured with an optical tachometer up to 500,000 rpm. For health protection reasons, the device includes a hinged safety guard.

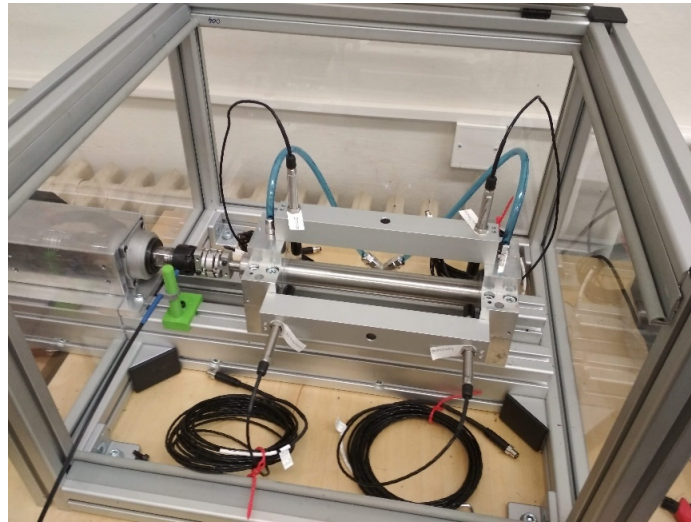


Fig. 1: Test rig for water-lubricated hydrodynamic journal bearings.

2.2 Measuring procedure

The speed maximum of 17,000 rpm was reached with a linear ramp in 120 s. The displacements of the journal were measured during the start-up, thanks to which the instantaneous position of the journal and its trajectory was determined. Fig. 2 presents a scheme of this measurement, including the used coordinate system. To compare measured data of the journal trajectory during the start-up with calculation, a computational model was created.

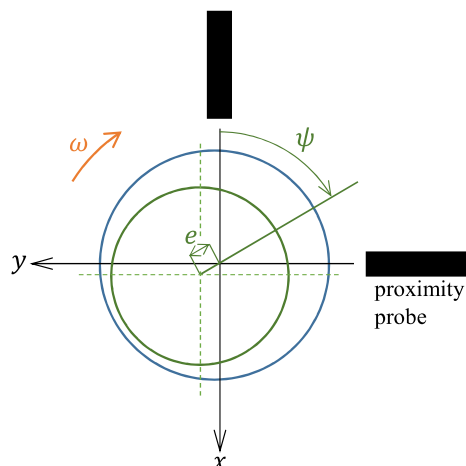


Fig. 2: Hydrodynamic journal bearing scheme with two proximity probes.

2.3 Computational model

The load-carrying capacity of a hydrodynamic bearing is given by the hydrodynamic pressure in the lubricant film. The computational model is therefore based on a numerical solution of the generalized Reynolds equation [14], which describes this pressure:

$$\frac{\partial}{\partial \theta} \left(\frac{H^3}{K_x} \bar{G} \frac{\partial \bar{p}}{\partial \theta} \right) + \frac{\partial}{\partial \bar{y}} \left(\frac{H^3}{K_y} \bar{G} \frac{\partial \bar{p}}{\partial \bar{y}} \right) = \frac{\partial}{\partial \theta} (\bar{G}_R H), \quad (1)$$

where $H = h/c_b$ is the dimensionless lubricant film thickness, $c_b = R - R_j$ is the radial assembly clearance, R is the bearing radius, R_j is the journal radius, $\bar{p} = pc_b^2/U\eta_0 R$ is the dimensionless pressure, U is the sliding velocity, η_0 is the initial dynamic viscosity, $\theta = x/R$ is the angular coordinate, $\bar{y} = y/R$ is the dimensionless axial coordinate, \bar{G} and \bar{G}_R characterize the variable lubricant viscosity and density, and K_x and K_y models effect of local turbulent flow and Taylor vortices. Detailed information is provided by the author in [1].

Due to the dissipation of energy in the lubricant film, the energy equation is solved simultaneously with the Reynolds equation, based on which the lubricant temperature can be determined. This is because the lubricant characteristics such as viscosity and density are temperature dependent. Dimensionless temperature distribution $T = T/T_0$ in the radial and circumferential directions of the lubricant film is expressed by the following energy equation:

$$\frac{\partial}{\partial \theta} (\bar{U} \bar{T}) + \frac{\partial}{\partial \bar{z}} (\bar{W} \bar{T}) = \frac{\partial}{\partial \theta} \left(\Lambda_\theta \frac{\partial \bar{T}}{\partial \theta} \right) + \frac{\partial}{\partial \bar{z}} \left(\Lambda_z \frac{\partial \bar{T}}{\partial \bar{z}} \right) + K_T \phi, \quad (2)$$

where T_0 is the water supply temperature, \bar{U} and \bar{W} are the modified dimensionless circumferential and radial velocities, Λ_θ and Λ_z are the modified dimensionless thermal diffusivities, K_T is the dissipation number, ϕ is the dissipation function, and $\bar{z} = z/h$ is the dimensionless radial coordinate (more details in [1]).

Due to the use of water as a lubricant, the effect of temperature is not as significant, unlike oil-lubricated bearings, whose viscosity is approximately two orders of magnitude higher. Nevertheless, the energy equation is given here for the model completeness.

The computational model further incorporates lubricant mixing, reaching a steady-state solution, tilting and deforming the pads with the subsequent establishment of the static equilibrium position of the journal [1]. This equilibrium position occurs once a balance is found between the external load and the hydrodynamic pressure resultant and the moment equilibrium of all segments with respect to the pivot is satisfied at the same time. The multidimensional root finding quasi-Newton method, namely the bounded Anderson method [1], is used to find the static equilibrium position of the bearing. This method and the used computational model are described in detail by the author [1].

3 Results

Tab. 1 summarizes the parameters of the investigated bearing.

Tab. 1: Characteristic data of the test bearing.

Number of tilting pads	3, load on pad
Bearing radius [mm]	15
Bearing length [mm]	18
Radial assembly clearance [μm]	25
Radial machined clearance [μm]	41
Pivot offset [-]	0.5
Rotational speed [rpm]	0–17,000
Bearing load [N]	8.2
Water supply temperature [$^\circ\text{C}$]	25

Fig. 3 shows hydrodynamic pressure distribution in the bearing mid-plane operating at a rotational speed of 2,000 rpm and 16,000 rpm. Maximum pressures are 66.7 kPa and 187.8 kPa. In addition to the pressure, Fig. 3 presents lubricant film thickness which is 50 times magnified. The film thickness at the lower pad increases with rotational speed. Minimum film thickness at 2,000 rpm and 16,000 rpm at the lower pad is $12.6 \mu\text{m}$ and $19.3 \mu\text{m}$, respectively. From the pads position, it is also evident that they are tilted into the converging wedge, which supports the formation of hydrodynamic pressure. Fig. 4 shows this pressure distribution in the circumferential and axial direction of the bearing. In the axial direction from the bearing mid-plane, hydrodynamic pressure decreases to atmospheric pressure, at which point lubricant leaves the bearing.

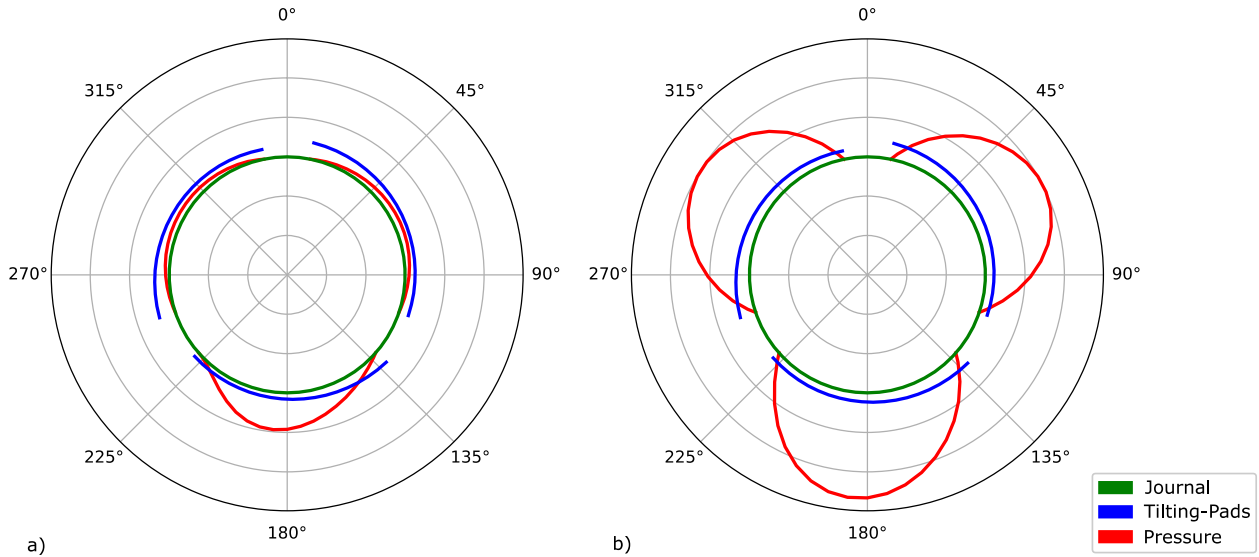


Fig. 3: Lubricant film thickness ($50\times$ magnified) and distribution of hydrodynamic pressure, (a) $n = 2,000$ rpm, (b) $n = 16,000$ rpm.

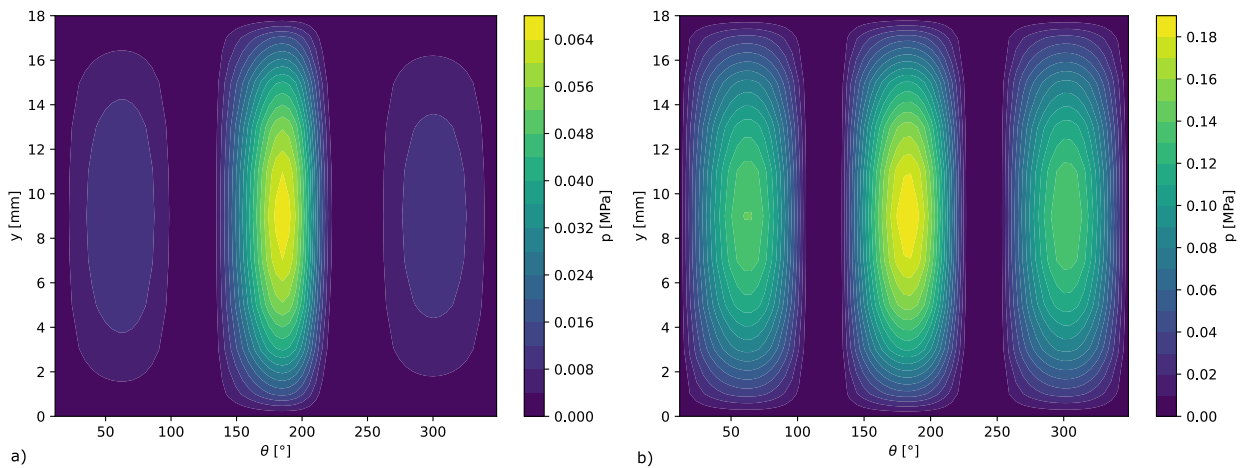


Fig. 4: Distribution of hydrodynamic pressure, (a) $n = 2,000$ rpm, (b) $n = 16,000$ rpm.

Fig. 5 presents the temperature change in the lubricant film and pads. Fig. 5 was scaled so that the lubricant film thickness was the same size as the thickness of the pads. The shaft temperature was assumed to be constant. The lowest temperatures are in the area of leading edges of the pads, the highest in the area of the trailing edges. The temperature distribution is almost the same on all the pads, which is due to the low external load on the journal in combination with relatively high rotational speed.

Fig. 6 shows the comparison of the measured and computed position of the journal center during start-up. The computational model works only with a fully developed hydrodynamic lubricant film, therefore the calculation cannot be performed at zero speed. In our case, the minimum rotational speed for the calculation was 80 rpm. At this speed, a very thin lubricant film of minimum thickness $1.8 \mu\text{m}$ was found, at which the bearing would not be possible to operate. Thus, the lower speeds were not considered only from the point of

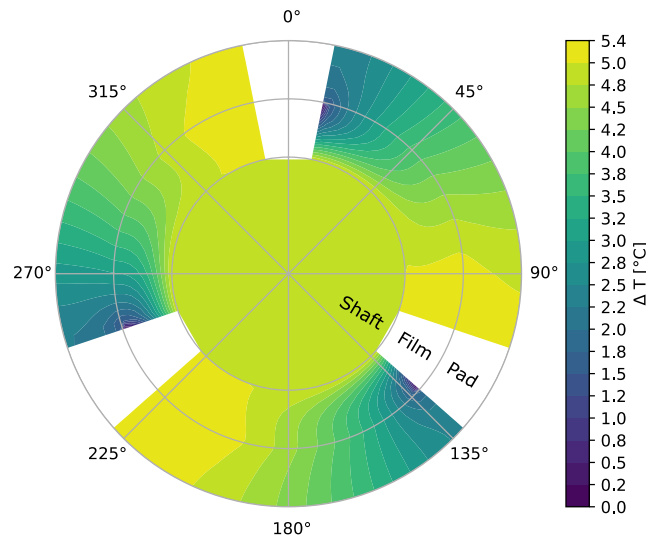


Fig. 5: Temperature change in the lubricant film and pads in the bearing mid-plane, $n = 16,000$ rpm.

view of the lubricant film thickness but also the point of view of the validity of the lubrication theory based on the Reynolds equation. Conversely, performing the measurement is not a problem without rotating the shaft. The biggest issue with the measurement is the noisy data, from which the noise needs to be removed. For this reason, a lowpass filter was used with a maximum rotational speed threshold. Furthermore, the data were approximated using least squares by a 6th order polynomial with fixed endpoints to gain the journal trajectory.

It can be stated that the difference between the calculated and measured data is not very large. At high speeds, the data almost match. In the region between approximately 2,000 rpm and 200 rpm, the calculated data deviates slightly in the y -direction. It is worth noting that the load on pad configuration does not have a clearly defined rest position of the rotor. Unlike the load between pads configuration where the rotor at rest lies between the pads. In the load on pad configuration, the rotor may lie to the left or right of the lower pad pivot and must first get out of this position when starting up. This corresponds to the initial part of the measured trajectory. The computational model is not able to capture this phenomenon, it determines the equilibrium position of the journal only after this transient process.

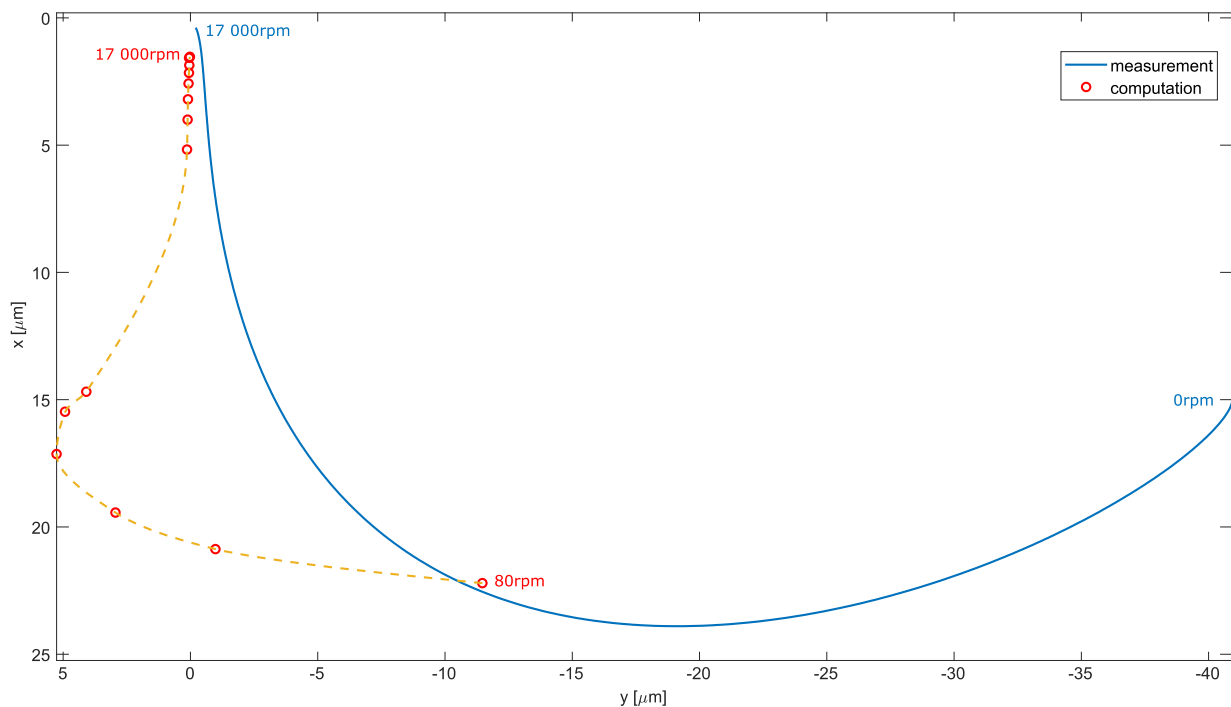


Fig. 6: Dependence of the journal locus on the rotational speed: a comparison of the computed and measured data.

4 Conclusion

The paper compared the measurement and calculation of the static equilibrium position of the water-lubricated tilting-pad journal bearing during rotor start-up. The test rig, its instrumentation and measuring procedure were presented. Furthermore, the computational model was given based on the generalized Reynolds equation solved simultaneously with the energy equation at the bearing mid-plane in the circumferential and radial direction. To find the equilibrium position, the model involved lubricant mixing, reaching the steady-state solution, tilting and deforming the pads.

To conclude, the comparison showed a good agreement between measurement and calculation at high speeds. The calculation could not be performed from the zero speed of the rotor because there is a minimum speed limit given by the full development of the lubricant film. In contrast, the measurement can be made in the rotor rest position. This position is not clearly defined in the load on pad configuration, which probably causes deviations in the results at lower speeds. However, other influences may play a role, such as the effect of the flexible coupling compensating for the misalignment of the rotating parts. Further research might be focused on the spring and damping coefficients of the hydrodynamic tilting-pad journal bearings due to their relationship to the static equilibrium position.

Acknowledgement

This work was partially supported by the project FV 21-23 funded by The Ministry of Education, Youth and Sports of the Czech Republic; and the project “Problems of the strength of materials and dynamics and their engineering applications” (FSI-S-20-6164).

References

- [1] J. Pokorný, An efficient method for establishing the static equilibrium position of the hydrodynamic tilting-pad journal bearings, *Tribol. Int.* 153 (2021), 106641, doi: [10.1016/j.triboint.2020.106641](https://doi.org/10.1016/j.triboint.2020.106641).
- [2] O. Reynolds, On the theory of lubrication and its application to Mr. Beauchamp tower’s experiments, including an experimental determination of the viscosity of olive oil, *Philos. Trans. R. Soc. London.* 177 (1886) 157–234, doi: [10.1098/rstl.1886.0005](https://doi.org/10.1098/rstl.1886.0005).
- [3] D. Dowson, A generalized Reynolds equation for fluid-film lubrication, *Int. J. Mech. Sci.* 4 (1962) 159–170, doi: [10.1016/S0020-7403\(62\)80038-1](https://doi.org/10.1016/S0020-7403(62)80038-1).
- [4] H.G. Elrod, C.W. Ng, A theory for turbulent fluid films and its application to bearings, *J. Tribol.* 89 (1967) 346–362, doi: [10.1115/1.3616989](https://doi.org/10.1115/1.3616989).
- [5] H. Heshmat, O. Pinkus, Mixing Inlet Temperatures in Hydrodynamic Bearings, *J. Tribol.* 108 (1986) 231–244, doi: [10.1115/1.3261168](https://doi.org/10.1115/1.3261168).
- [6] C.M.M. Ettles, The analysis and performance of pivoted pad journal bearings considering thermal and elastic effects, *J. Tribol.* 102 (1980) 182–191, doi: [10.1115/1.3251465](https://doi.org/10.1115/1.3251465).
- [7] J. Pokorný, Calculation of Static Equilibrium Position of Hydrodynamic Journal Bearings, in: *Eng. Mech.* (2019), Czech Academy of Sciences, Svratka, 291–294, doi: [10.21495/71-0-291](https://doi.org/10.21495/71-0-291).
- [8] W. Zhou, X. Wei, L. Wang, G. Wu, A superlinear iteration method for calculation of finite length journal bearing’s static equilibrium position, *R. Soc. Open Sci.* 4 (2017), doi: [10.1098/rsos.161059](https://doi.org/10.1098/rsos.161059).
- [9] S. Yu, S. Chen, An approach searching for the steady-state equilibrium position of tilting-pad journal bearing for supporting motorized spindle, *J. Comput. Theor. Nanosci.* 9 (2012) 1710–1714, doi: [10.1166/jctn.2012.2269](https://doi.org/10.1166/jctn.2012.2269).
- [10] A. Cerda Varela, B. Bjerregaard Nielsen, I.F. Santos, Steady state characteristics of a tilting pad journal bearing with controllable lubrication: Comparison between theoretical and experimental results, *Tribol. Int.* 58 (2013) 85–97, doi: [10.1016/j.triboint.2012.10.004](https://doi.org/10.1016/j.triboint.2012.10.004).

- [11] S. Taniguchi, T. Makino, K. Takeshita, T. Ichimura, A thermohydrdynamic analysis of large tilting-pad journal bearing in laminar and turbulent flow regimes with mixing, *J. Tribol.* 112 (1990) 542–550, doi: [10.1115/1.2920291](https://doi.org/10.1115/1.2920291).
- [12] T. Hagemann, S. Kukla, H. Schwarze, Measurement and prediction of the static operating conditions of a large turbine tilting-pad bearing under high circumferential speeds and heavy loads, in: *Proc. ASME Turbo Expo*, 2013, doi: [10.1115/GT2013-95004](https://doi.org/10.1115/GT2013-95004).
- [13] K.D. Wygant, R.D. Flack, L.E. Barrett, Measured Performance of Tilting-Pad Journal Bearings over a Range of Preloads—Part I: Static Operating Conditions, *Tribology Transactions*. 47 (2004) 576–584, doi: [10.1080/05698190490504154](https://doi.org/10.1080/05698190490504154).
- [14] N. Mittwollen, J. Glienicke, Operating conditions of multi-lobe journal bearings under high thermal loads, *J. Tribol.* 112 (1990) 330–340, doi: [10.1115/1.2920261](https://doi.org/10.1115/1.2920261).